The relation between land use and subsidence in the Vietnamese Mekong delta

P.S.J. Minderhoud [a,b,*], L. Coumou [a], L.E. Erban [c], H. Middelkoop [a], E. Stouthamer [a], E.A. Addink [a]

[a] Department of Physical Geography, Utrecht University, Utrecht, The Netherlands
[b] Department of Subsurface and Groundwater Systems, Deltares Research Institute, Utrecht, The Netherlands
[c] US EPA Office of Research and Development, National Health and Environmental Effects Research Laboratory, Atlantic Ecology Division, Narragansett, RI, USA

HIGHLIGHTS

- Land-use practices can influence subsidence processes, amplifying natural subsidence or inducing anthropogenic subsidence.
- We assess the relation between land use and subsidence using land-use time series and InSAR-derived subsidence rates.
- Different land-use classes are experiencing different rates of subsidence.
- Highest subsidence rates were found for land-use classes in which natural conditions were most altered by human activities.
- Land use and land-use history have an indirect, causal relationship with subsidence rates in the Mekong delta.

GRAPHICAL ABSTRACT
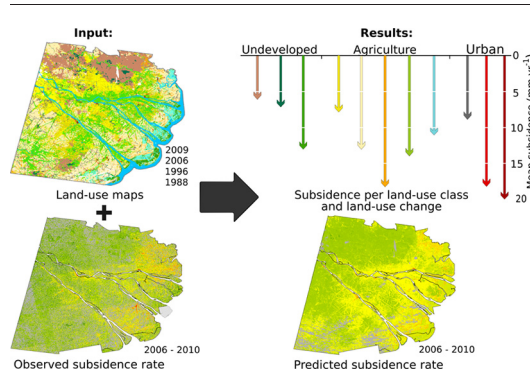
ARTICLE INFO

ABSTRACT

The Vietnamese Mekong delta is subsiding due to a combination of natural and human-induced causes. Over the past several decades, large-scale anthropogenic land-use changes have taken place as a result of increased agricultural production, population growth and urbanization in the delta. Land-use changes can alter the hydrological system or increase loading of the delta surface, amplifying natural subsidence processes or creating new anthropogenic subsidence. The relationships between land use histories and current rates of land subsidence have so far not been studied in the Mekong delta.

We quantified InSAR-derived subsidence rates for the various land-use classes and past land-use changes using a new, optical remote sensing-based, 20-year time series of land use. Lowest mean subsidence rates were found for undeveloped land-use classes, like marshland and wetland forest (~6–7 mm yr^{-1}), and highest rates for areas with mixed-crop agriculture and cities (~18–20 mm yr^{-1}). We assessed the relationship strength between current land use, land-use history and subsidence by predicting subsidence rates during the measurement period solely based on land-use history. After initial training of all land-use sequences with InSAR-derived subsidence rates, the land-use-based approach predicted 65–92% of the spatially varying subsidence rates within the measurement error range of the InSAR observations (RMSE = 5.8 mm). As a result, the spatial patterns visible in the observed subsidence can largely be explained by land use. We discuss in detail the dominant land-use change pathways and their indirect, causal relationships with subsidence. Our spatially explicit evaluation of these

* Corresponding author at: Department of Physical Geography, Utrecht University, Utrecht, The Netherlands.
  E-mail address: p.s.j.minderhoud@uu.nl. (P.S.J. Minderhoud).

pathways provides valuable insights for policymakers concerned with land-use planning in both subsiding and currently stable areas of the Mekong delta and similar systems.

1. Introduction

Many of the world's major deltas have experienced significant anthropogenic change during the past decades. Within Southeast Asia, the Vietnamese Mekong delta stands out as hotspot of anthropogenic land-use change (Giri et al., 2003). Following Vietnam's transition towards an open-market economy in 1986, the vast majority of natural wetlands and forested areas in the delta have been converted to agricultural lands dominated by rice paddies (Funkenberg et al., 2014; Tran et al., 2015). Along the Mekong river branches, orchards and fish farms have been created, and in the coastal zone vegetables farms sprouted on the higher elevated beach ridges. Furthermore, mangroves have been cut to make place for shrimp farms and other aquaculture (a. o. Binh et al., 2005; Sakamoto et al., 2009; Tong et al., 2004). Over the years, rice production in the delta has increased as intensified irrigation allowed for more crops per year (Sakamoto et al., 2006). Moreover, the delta has become progressively urbanized, with an ever-densifying and expanding network of roads connecting the fast-growing settlements, cities and industrial areas (Karila et al., 2014; Tran et al., 2015). Other large-scale alterations of the delta system include increased flood control through extensive dike systems (Triet et al., 2017), sand mining activities in the river branches (Brunier et al., 2014), and wide-spread exploitation of groundwater resources (Wagner et al., 2012). The Vietnamese Mekong delta is further impacted by reduced sediment supply due to upstream dams (Kummu and Varis, 2007; Kondolf et al., 2014), decreased hurricane activity (Darby et al., 2016), salinization (Renaud et al., 2015), coastal erosion (Anthony et al., 2015) and global sea-level rise in response to climate change (Wassmann et al., 2004). On top of that, the delta is subsiding at rates up to several centimeters a year, exceeding current absolute sea-level rise by up to a magnitude (Erban et al., 2014; Minderhoud et al., 2017).

Land subsidence is a natural phenomenon in delta systems. Deltaic sediments are highly compressible and susceptible to significant natural compaction during deposition and subsequent soil formation. Enhanced land subsidence in deltas due to human activities is widely recognized (e.g. Syvitski et al., 2009; Giosan et al., 2014). Human use of land and groundwater resources can amplify natural subsidence processes or initiate new anthropogenic subsidence in different ways (Galloway et al., 2016). Firstly, subsidence can be enhanced by direct loading of the delta surface, both by natural material, such as water and sediment, and by anthropogenic artifacts, such as buildings and infrastructure. Secondly, drainage of wetlands to prepare for agricultural use leads to a lowering of the phreatic water table, causing compaction and aeration of the subsoil. Consequent decomposition of organic material (oxidation) causes additional volume reduction (e.g. Van Asselen et al., 2009). Additionally, the extraction of groundwater from deeper aquifers (water-bearing sediment layers), to meet the increasing freshwater demands of rapidly urbanizing areas, agriculture and aquaculture, can trigger aquifer-system compaction (e.g. Galloway and Burbey, 2011; Gambolati and Teatini, 2015). In the Vietnamese Mekong delta evidence of widespread absolute subsidence was recently revealed by InSAR (Interferometric Synthetic Aperture Radar) (Erban et al., 2013, 2014). Minderhoud et al. (2017) demonstrated that a steady increase of groundwater use and excessive pumping over the past decades has dramatically accelerated subsidence in this area. Together, these land-use developments of the past decades in the Vietnamese Mekong delta have affected the natural environment, and introduced anthropogenic drivers, enhancing subsidence rates.

Subsidence is a sluggish process that may show a remarkably slow but pertinent response to a change in land use, due to time-dependent

effects of both subsidence *drivers* and *processes*. For example, the amount of groundwater extraction (*driver*) might grow gradually over the years following a change in land use. The consequent aquifer-system compaction (*process*) increases even more slowly, as it takes time for overpressure to dissipate from clay-rich sediments which than start to compact and due to time-dependent secondary consolidation. This process can continue up to decades after initiation. This implies that groundwater extractions under past land use still can affect present-day subsidence rates; hence land use and land use history might be important indicators of present-day subsidence rates in a delta.

In this study, we aim to quantify the relationship between land use and land subsidence rates and to determine the effect of past land-use changes in the Vietnamese Mekong delta. We hypothesize that land use and land-use history correlate to subsidence in two ways: 1) by affecting subsidence drivers and processes as described above, and, 2) through location preference of certain land-use types for a geomorphological setting with specific subsidence characteristics, e.g. orchards prefer higher elevated, sandy natural levees, which are less prone to shallow compaction. Thus, land use could potentially explain part of the spatial patterns of observed subsidence rate and may serve as an indirect proxy for subsidence rate. We used optical remote sensing-based products to map land use and land-use change, together with InSAR-derived subsidence rates for a representative part of the Mekong delta. We created a time series of land use from Landsat TM5 images and determined subsidence rates for specific land-use sequences both for areas with unchanged land use in the period 1988–2006, and for areas in which land-use changes occurred during this period. Subsequently, we assessed the impact of land use and land-use changes on subsidence rates and derive time-dependent effects of subsidence. Moreover, we evaluate the strength of the relationship between land use and subsidence rate by predicting and mapping subsidence rate solely based on land use and land-use history. The ability to predict subsidence rates based on land use and land-use history, after the initial training of individual land-use change sequences with observed subsidence rates, reveals the relation between land use and subsidence in the Mekong delta.

2. Data and methods

2.1. Consistent land-use time series

A consistent land-use time series of the Mekong delta over the past decades is required to study the relation between land use, land-use change and subsidence rates. The Vietnamese government produces land-use maps every five years (Dijk et al., 2013; Phuong and Catacutan, 2014), but they are not publicly accessible and, if available, lack metadata on data sources and used methods. Besides these national maps, many land-use maps exist for the Mekong delta, however they all vary in terms of *subject* (e.g. rice cropping system: Bouvet and Le Toan, 2011; Karila et al., 2014; Kono, 2001; shrimp farm expansion: Giang and Hoa, 2013; Tong et al., 2004; Vo et al., 2013), *spatial extent* (regional: e.g. Chen et al., 2012; delta-wide: e.g. Sakamoto et al., 2006, 2009; Son et al., 2013 and Xiao et al., 2006), *defined land-use classes* (Kuenzer et al., 2011), *used satellite imagery* (MODIS (e.g. Kuenzer and Knauer, 2013), SPOT (e.g. Nguyen et al., 2012), Landsat (e.g. Funkenberg et al., 2014) or Rapid Eye (e.g. Huth et al., 2012)) and *classification method and accuracy* (Kuenzer et al., 2011; Kuenzer and Knauer, 2013). Consequently, no single study or combination of studies provided a consistent land-use time series of the Mekong delta appropriate for our study.

2.1.1. Land-use mapping

We created a new consistent time series of land-use maps using optical remote sensing Landsat Thematic Mapper (TM) 5 images. Landsat TM5 imagery was selected for its long period of available images (1984–2013), the large range of spectral bands, the suitable ground resolution (30 m) for land-use mapping and free of charge availability (see Supplementary Information (SI), section S1.1). The Landsat tile with the largest spatial coverage of the delta was selected as study area (WRS path 134, row 053, Fig. 1). This area hosts all major land-use types present in the Mekong delta. We selected four images with limited cloud cover acquired during the dry season (January – March) in 1988, 1996, 2006 and 2009 to enable distinction of dry-season irrigation.

For our analyses we defined land-use classes that 1) encompassed all land-use types representative for the entire delta, 2) were identifiable from the Landsat 5 TM images and 3) were potentially related to different subsidence drivers. We considered the characteristics of all land-use classes regarding the following three main human-induced subsidence drivers associated with land-use practices: 1) lowering of the phreatic water table, 2) extracting groundwater and 3) loading of the delta surface by buildings and infrastructure (Table 1). Unlike other land-use studies in the Mekong delta, we did not distinguish rice agriculture based on the number of annual crops, for this could not be determined based on a single, dry-season image. Nevertheless, rice crop phenology patterns (Son et al., 2014) do indicate that our

land-use class "dry-season rice" likely corresponds to two or three annual irrigated rice crops and 'dry season bare field' to one or two annual rain-fed crops.

2.1.2. Object-based image analysis

The Landsat images were classified using object-based image analysis (OBIA) (Addink et al., 2012). This means that neighboring pixels in the images are grouped into objects ("segmentation"), which are subsequently classified based on object characteristics. The large advantage of OBIA over more traditional, pixel-based classification is that not only spectral, but also shape and context characteristics can be used for the classification (Addink et al., 2012). This enables the distinction of different land-use classes with similar land cover and hence spectral behavior in the Landsat images. For example, a shrimp pond and a canal both have the spectral properties of water. However, with OBIA they can be distinguished based on their shape, e.g. rectangular versus a line. As a result, OBIA generally performs better than pixel-based approaches, especially with high-resolution imagery (Blaschke, 2010).

As preprocessing step, we created a shapefile outlining clouds and cloud shadows in each image. In this step, each image was segmented and classified using the seven Landsat 5 TM spectral bands, the enhanced vegetation index (EVI), the normalized difference vegetation index (NDVI) and the normalized difference moisture index (NDMI) (see SI S1.2.1. for detailed description of the process and segmentation
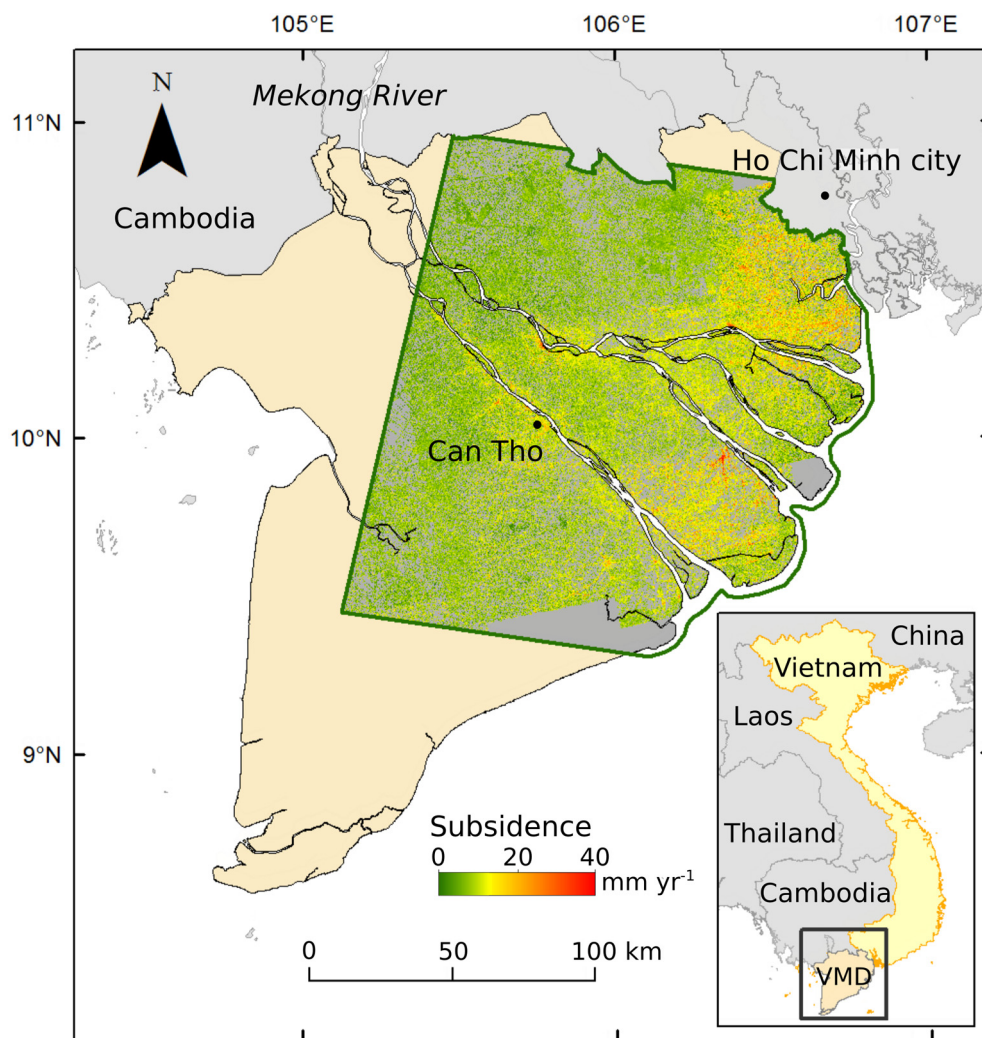
Fig. 1. The location of the study area (outlined in green) with InSAR-derived subsidence rates in the Vietnamese Mekong delta (VMD) in Southeast Asia. The selected area corresponds to the Landsat 5 TM tile: WRS path 134, row 053 (USGS, 2016) and has an area of ~20,000 km². Subsidence rates are InSAR-derived annual means for 2006–2010 (Erban et al., 2014). (For interpretation of the references to color in this figure legend, the reader is referred to the web version of this article.)

Table 1
Land-use classes used for the classification and their estimated characteristics related to subsidence.

Land-use class	Land-use practices related to subsidence		
	Phreatic water table	Groundwater use	Anthropogenic loading
Marshland/marshes	High, year-round	–	–
Wetland forest[a]	High, year-round	–	–
Mangroves	High, year-round	–	–
Dry-season rice (*irrigated rice; two or three crops yr^{-1}*)	High, year-round (excl. harvest)	–[b]	–
Dry-season bare field (*rain fed rice; one or two crops yr^{-1}*)	Wet- and dry-season fluctuation	–	–
Dry-season partly rice (alternation rice and bare field)[c]	Wet- and dry-season fluctuation	–[b]	–
Mixed crops – non-rice	Lowered by drainage	Moderate-High	–
Orchard	Lowered by drainage	Low-Moderate	–
Aquaculture (mainly shrimp farming)	Wet- and dry-season fluctuation	Moderate-High	–
Linear settlements[d]	Wet- and dry-season fluctuation	Low-Moderate	Moderate
Urban dense	Lowered by drainage	High	High
Urban open	Lowered by drainage	High	High
Water: sea, rivers, small channels			
Clouds			

[a] Based on other land-use maps, "wetland forest" is dominated by melaleuca trees, but other tree species may be present.
[b] Groundwater use for rice irrigation is prohibited by Vietnamese law. Rice is irrigated using surface water.
[c] The classification aims at classifying land-use at delta scale and therefore, relatively small-scale inter-field alternations between the "dry season rice" and 'dry season bare field' class are merged as one class: "Dry season partly rice".
[d] Linear settlements are narrow settlements or groups of buildings stretched along a transport route, like a road or canal. They are the common form of settlement in the rural parts of the Mekong delta.

settings). The classification result was subsequently used to mask the clouds and cloud shadows in the Landsat images. Subsequently, each cloud-masked Landsat image was segmented using six Landsat 5 TM spectral bands (thermal infra-red was excluded because of its coarser resolution and limited value for land-use discrimination), the EVI and the NDMI. Pixels were grouped based on their spectral resemblance aiming at maximum within-object spectral similarity (see SI S1.2.2. for details). After segmentation, a large random selection of objects ($n =$ 1100) was manually labelled to the corresponding land-use class to serve as training and validation datasets.

2.1.3. Land-use classification

We employed a "random-forest" algorithm to assign the land-use classes to the segments in the Landsat images (Gislason et al., 2006; Rodriguez-Galiano et al., 2012). A random forest is a data-mining or machine learning method that uses an ensemble of decision trees (the "forest") to "predict" land-use class using multiple object variables (here spectral, shape and context characteristics of the object). We used the randomForest package v. 4.6–12 in R v 3.3.2 (Breiman and Cutler, 2003). Random forests are insensitive to noisy input data and make no assumptions about the frequency distribution of training samples (Funkenberg et al., 2014). Besides they correct for potential overfitting of a single decision tree (Breiman, 2001).

The randomly selected training-and-validation dataset was split randomly into a training (2/3) and validation set (1/3). The training set was used to train a random forest, containing 10,000 decision trees, with 55 object features as input variables and the land-use classes as output variable (SI, Table A4). The trained random forest was subsequently used to classify all objects of the image based on their spectral and spatial characteristics. This procedure was repeated for each Landsat image to create four consistent land-use maps. The land-use map of 2009 suffered from extensive cloud cover, which would greatly reduce the size of the area for analysis. Moreover, comparison between the 2006 and 2009 land-use map revealed few differences. Therefore, we excluded the land-use map of 2009 from further analyses and adopted the land-use map of 2006 as representative for the period during which the InSAR-based subsidence rates were estimated (2006–2010). From the three remaining maps, we created maps that indicate the land-use sequence from 1988 to 2006. For complete description of the land-use classification procedure, pre- and post-processing steps and validation, see Supplementary Information (SI, section S1.2).

2.2. InSAR-derived subsidence rates

The InSAR-derived (Interferometric Synthetic Aperture Radar) subsidence rates by Erban et al. (2013, 2014) are the first, and until present only, available estimates of subsidence providing spatial coverage for large parts of the Vietnamese Mekong delta. The subsidence rate estimates are based on the phase shift in radar returns from coherent reflectors at the earth surface or from areas where the surface texture remains largely unchanged during the study period. Examples include roads and rooftops, which are well distributed throughout the delta in urban and rural areas. Subsidence rates are not estimated for pixels with low InSAR correlation. Changes in surface elevation due to flooding and associated sediment aggradation therefore cannot be detected using InSAR, as areas subject to these changes exhibit low InSAR correlation. As a result, the subsidence-rate estimates do not provide continuous spatial coverage. Furthermore, as sediment aggradation is not included, the quantified rates represent subsidence rather than net surface elevation change. The InSAR raster dataset (spatial resolution ₋57 × 57 m) represents mean subsidence rates for the period 2006–2010 (in mm yr^{-1}), with an estimated error due to spatio-temporal variability in surface scattering properties of 5–10 mm yr^{-1} (Erban et al., 2013). The rasters were georectified, mosaicked and a subset was created for the extent of the study area (Fig. 1).

2.3. Relating land use and land-use change to subsidence

The land-use-sequence maps were combined with the InSAR-based subsidence rates to quantify subsidence rates for individual land-use sequences. First, the InSAR raster dataset was converted to a point dataset with a point in the center of each grid cell. Then, the InSAR points corresponding to each land-use-sequence object were extracted and their median subsidence value was assigned as representative object-subsidence rate.

Four categories of land-use sequences can be distinguished. The first category comprises the constant-land-use sequences, i.e. land use remained the same from 1988 until 2006. The second category comprises the sequences where a land-use conversion occurred between 1988 and 1996, but no conversion took place between 1996 and 2006. The third category is the inverse of the second and in the fourth category during both periods a change occurred. This resulted in a map with segments representing unique sequences of 3 land use

types that occurred in the three periods. We focused on the first, second and third category (sequence category 1, 2 and 3), i.e. where the land-use sequences contain at most one change in land-use.

We compared subsidence rates for the first three categories (category 1, 2 and 3) of land-use sequence to determine the relation between land use and subsidence. For each land-use sequence the subsidence rates in all composing objects with this sequence were determined, and the median value of these rates was taken to obtain the characteristic land-use-sequence subsidence rate. The subsidence rates for the sequence category without land use change were considered to represent the primary relation between land use and subsidence rate. By comparing these subsidence rates with those for the other two categories of sequences (with land-use change), we determined a potential time-lag effect in the response of subsidence rate to land-use change. So, for example, we compared subsidence rates for the marshland-changed-to-rice sequences (sequence categories 2 and 3) with those for areas that where marshland and rice fields during the entire period (both first sequence category). For these analyses, we focused on the prominent and characteristic land-use sequences that reflect the developments in the delta, which are: cultivation of previously undeveloped land, changes in agricultural practice, and urbanization.

2.4. Predicting subsidence rates based on land-use sequence

We evaluated the strength of the relationship between land use, land-use change and subsidence according to the ability to predict subsidence rates based solely on land-use history. For each unique sequence, two thirds of the objects were assigned to a training set and one third to a validation set. All objects classified as water in any year were excluded. For each unique land-use sequence we determined the median InSAR-based subsidence rate of all comprising objects. Next, a subsidence prediction map was made by assigning the median rate of each land-use sequence to every individual object. From the resulting map the independent validation objects were retrieved and their InSAR-based subsidence observation was compared to the land-use predicted value. To test the added value of including land-use history and not just land use in the analysis, we also created a prediction map based only on the land use map of 2006 for comparison.

3. Results

3.1. Land-use maps and land-use change

The land-use maps for 1988, 1996, 2006 and 2009 based on the Landsat TM5 images are shown in Fig. 2; the areal coverage of each land use class is shown in SI, Fig. A2. None of the maps is completely cloud-free, but the 2009 land-use map suffers from extensive cloud cover (>26%). The overall accuracies of the land-use maps are 77%, 94%, 92% and 89% for the land-use maps of 1988, 1996, 2006 and 2009 respectively (SI, table A5).

Between the years 1988, 1996 and 2006, major changes in land use occurred, and by the year 2006 only 30% of the area land use had remained unchanged since 1988 (Table 2). The total area of undeveloped land (i.e. marshland, wetland forest and mangroves) strongly decreased from 18% to 5% between 1988 and 2006. The total area used for rice production (i.e. "dry-season bare field", "dry-season partly rice", "dry-season rice") remained stable throughout this period, and covered over half of the entire study area. The area used for other agricultural practices (orchards and mixed crops) strongly increased between 1988 and 1996, but decreased again towards 2006, while aquaculture and urbanized areas steadily increased in size from the start of the study period until 2006. These developments directly reflect population growth and urbanization of the Mekong delta during the past decades

with growing delta cities and more shrimp farms as response to increased salinization.

The transition matrices for the periods 1988–1996 (Table 3) and 1996–2006 (Table 4) provide a quantitative overview of the land-use changes. The most prominent change that took place is the expansion of irrigated rice culture (class "dry-season rice") by reclaiming marshland and intensifying rice production that previously were rain-fed ('dry-season partly rice' and 'dry-season bare field'), especially between 1988 and 1996. Along the main river braches, orchards expanded at the expense of "dry-season rice". Furthermore, along the coast mangroves were cut to make place for aquaculture. The area of wetland forest strongly increased between 1996 and 2006 at the expense of marshlands, reflecting natural succession or anthropogenic conversion to forested lands. Finally, urban areas expanded, as well as rural settlements that appeared as linear elements throughout the delta.

### 3.2. Subsidence rates per land-use class

InSAR-based subsidence rates (measured by InSAR between 2006 and 2010) of all points for each land use class that did not change during the period 1988–2006 are shown in Fig. 3. Lowest subsidence rates occurred in undeveloped marshland with a mean rate of 6 mm yr^{-1}, closely followed by wetland forest (7 mm yr^{-1}). The highest subsidence rates were found for agricultural areas with mixed crops and urban areas (respectively 18 and 20 mm yr^{-1}). The within-class variability of subsidence rates varies with standard deviations between 4 mm yr^{-1} (marshland and wetland forest) and 7 mm yr^{-1} (several agriculture land-use classes, aquaculture and mangroves) (SI table A10). Differences in median and mean subsidence rates larger than 1 mm yr^{-1} between classes are significant (SI, section S3.2).

3.3. Relation between land-use change and subsidence rate

The effects of past land-use change on modern subsidence rates were assessed for three typical development groups (Table 5), which are 1) cultivation of previously undeveloped land, 2) changes in agricultural practice, and 3) urbanization. Areas where undeveloped land was reclaimed for cultivation, and where urbanization occurred generally experienced higher subsidence rates. Areas where changes between agricultural practice occurred experienced higher or lower subsidence rates, depending on the specific land-use change. Furthermore, where land use already changed to its current type in the first period (1988–1996) current subsidence rates are closer to those of the unchanged land-use sequence, than where the change occurred in the second period (1996–2006). Remarkably, highest subsidence rates are found in the areas where land use changed into "urban dense" between 1988 and 1996, exceeding the rates found for the unchanged "urban dense" sequence.

3.4. Predictions of subsidence rate based on land-use history

The land-use based predictions of land subsidence rates for the period 2006–2010 show spatial patterns similar to those derived from InSAR, with increasing rates from northwest to southeast and aligned along the river branches (Fig. 4A/B). The predicted subsidence rates show a strong linear relation with the InSAR rates and no bias (regression equation: slope = 0.99, intercept = 0.02, $r^2 = 0.16$: SI Fig. A4). As the predictions use a single, median subsidence rate for each land-use sequence that is attributed to the objects, the resulting subsidence estimation map is more uniform than the map of InSAR-observed rates. The root mean squared error (RMSE) between observed and estimated rates is 5.8 mm yr^{-1}. If we consider the InSAR estimated error range of the observed subsidence rates (5 to 10 mm yr^{-1}), 65% to 92% of the predictions are within range with the observed InSAR values (Fig. 4C). The spatial patterns and trends present in the InSAR and predicted subsidence rate maps are not visible anymore in the residuals
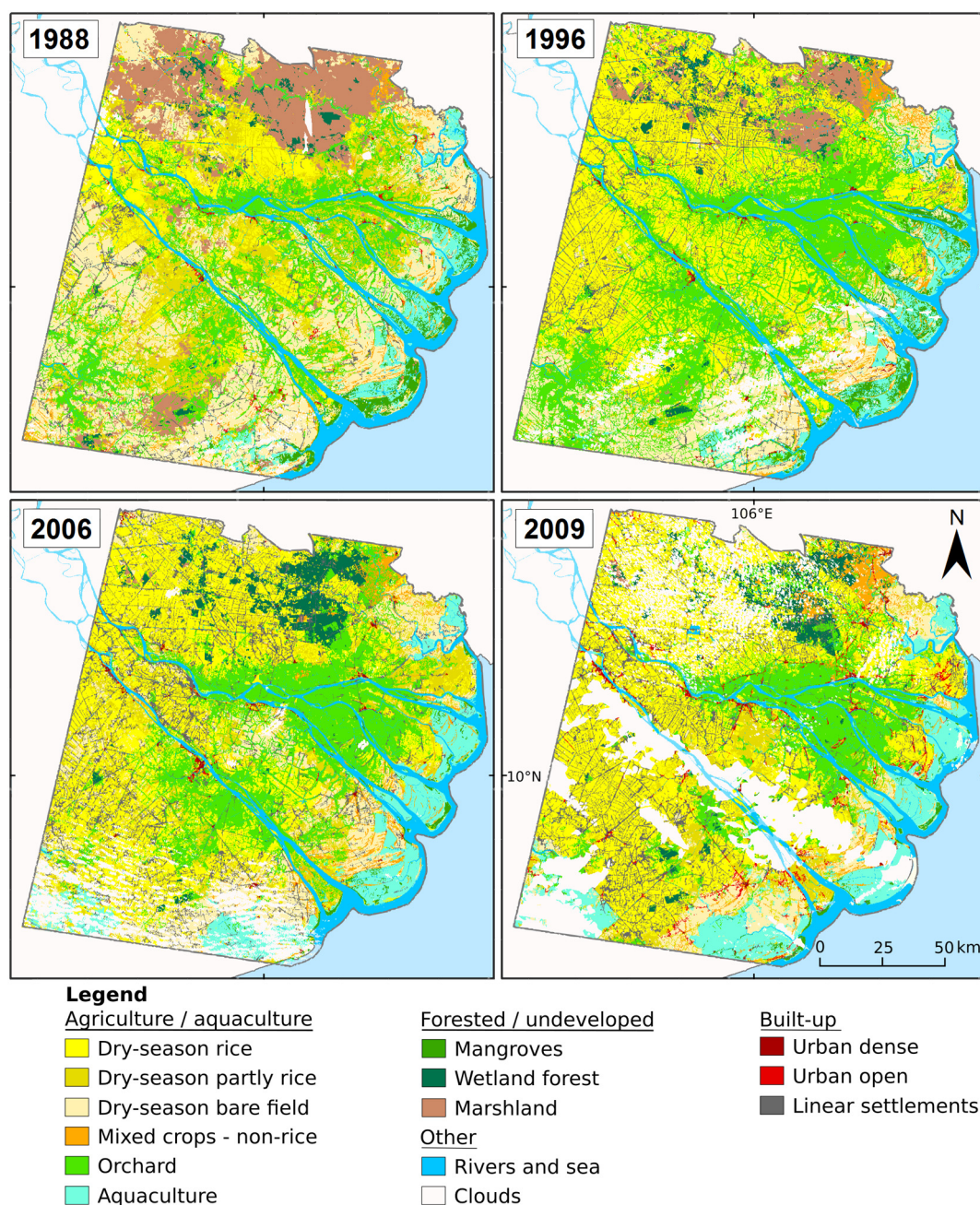
Fig. 2. Land-use maps of the northeastern part of the Vietnamese Mekong delta derived from Landsat 5 TM imagery of 1988, 1996, 2006 and 2009. The "dry-season rice" class represents irrigated rice cultivation producing two or three annual rice crops, while 'dry-season bare field' is rain-fed rice with one or two annual rice crop(s). 'Dry-season partly rice' represents small-scale patchwork of rice crops and bare field.

(Fig. 4C). When the prediction is only based on present land use without including land-use history, the correlation of the predicted subsidence and the observed subsidence decreases ($r^2 = 0.09$).

Table 2
Total area of main land-use classes in the land-use maps of 1988, 1996 and 2006. Area is color-coded from green (small) to red (large) and given in percentage of the total study area excluding cloud-covered areas.

	Land-use maps		
Main land-use classes	**1988**	**1996**	**2006**
Undeveloped	18	9	5
Rice	54	50	54
Other agriculture	21	32	23
Aquaculture	4	4	8
Urban	3	5	10

4. Discussion

4.1. Land-use change

Land-use changes show a trend of expansion and intensification of rice agriculture, aquaculture expansion at the expense of mangroves, and urbanization of the Vietnamese Mekong delta. These trends are in agreement with spatial and temporal patterns reported in other studies (e.g., Sakamoto et al., 2009; Tran et al., 2015). The timing of the widespread marshland cultivation (1988–1996) coincides with the economic and political reforms following the transition of Vietnam towards an open-market economy in 1986 (Funkenberg et al., 2014). The spatial pattern of the land-use class "dry-season rice" largely agrees with the extent of irrigated double and triple rice cropping areas, while 'dry-season bare field' agrees with the extent of rain-fed single and double rice

Table 3
Land use and land-use changes: 1988 and 1996. Area is color-coded from green (small) to red (large) and given in percentage of the total study area excluding cloud-covered areas. Land use remained unchanged in 42% of the study area (*in italic* the percentage of unchanged land-use area). Blank spaces show land-use changes that did not happen.

		Aqua-culture	Dry-s. rice	Dry-s. p. rice	Dry-s. b. field	Mix c. no rice	Mangroves	Wet. Forest	Orchard	Urban dense	Urban open	Linear Settle.	Water	Marsh-land	Total in 1988
								Land-use class in 1996							
Land-use class in 1988	Aquaculture	*2.4*	0.0	0.0	0.1	0.0	0.6		0.1	0.0		0.0	0.1	0.0	3.4
	Dry-season rice	0.0	*7.1*	0.1	0.1		0.0	0.0	1.2	0.0	0.0	0.5	0.0	0.0	9.1
	Dry-season partly rice	0.1	6.5	*0.7*	0.6	0.2	0.1	0.2	7.7	0.0	0.1	1.0	0.1	0.2	17.4
	Dry-season bare field	0.4	8.6	1.5	*7.3*	0.5	0.3	0.0	3.5	0.1	0.1	0.8	0.1	0.1	23.2
	Mix crops - non-rice	0.1	0.1	0.1	0.2	*0.6*	0.1	0.0	0.3			0.1	0.0	0.1	1.6
	Mangroves	0.6	0.0	0.0	0.1	0.0	*1.1*		0.2			0.0	0.0		2.1
	Wetland forest	0.0	0.2	0.0	0.0	0.0		*0.4*	0.1			0.1	0.0	0.3	1.1
	Orchard	0.1	3.8	0.4	0.3	0.2	0.3	0.3	*11.5*	0.0	0.0	0.8	0.2	0.1	17.8
	Urban dense		0.0	0.0						*0.0*	0.0	0.0			0.1
	Urban open	0.0	0.0	0.0	0.0	0.0			0.1	0.0	*0.0*	0.0	0.0	0.0	0.3
	Linear settlement	0.0	0.7	0.1	0.2	0.1	0.0	0.0	0.4	0.0	0.0	*0.5*	0.0	0.0	2.1
	Water	0.4	0.1	0.0	0.0	0.0	0.1	0.0	0.3	0.0	0.0	0.1	*7.2*	0.0	8.3
	Marshland	0.0	5.5	0.4	0.5	0.3	0.0	0.9	1.6	0.0	0.0	0.7	0.1	*3.4*	13.6
	Total in 1996	4.0	32.6	3.4	9.7	1.9	2.5	1.9	27.1	0.2	0.2	4.5	7.9	4.2	100.0

crops (e.g. Son et al., 2014; Sakamoto et al., 2009). Furthermore, the rice farming intensification, to enable the growth of an additional rice crop per year, is clearly shown by the consecutive land-use maps characterized by the expansion of the dry-season, hence irrigated rice. This is especially apparent in the upstream part of the delta. The large-scale transition of mangroves to aquaculture in the coastal zone observed between 1996 and 2006 is in line with Binh et al. (2005), Karila et al. (2014), Sakamoto et al. (2009b) and Tran et al. (2015). The steady increase of linear settlements along channels, dikes and roads, as well as urban areas, corresponds with the findings of e.g. Binh et al. (2005) and Tran et al. (2015).

4.2. Land-use driven subsidence

The main anthropogenic subsidence drivers associated with land-use practices are lowering of the phreatic water table, groundwater extraction and loading of the delta surface by buildings and infrastructure (e.g. Minderhoud et al., 2015; Galloway et al., 2016). We ranked the land-use classes by their mean observed subsidence rate (Fig. 5), and qualitatively estimated the impact of each subsidence driver for each

land-use class based on the characteristics as described in Table 1. To exclude the influence of time lags of subsidence following a land-use change in the studied period, the subsidence rate per land-use class was based on areas that sustained the same land use throughout the period of 1988–2006 (Fig. 3). A trend is apparent between anthropogenic impact on the natural system and the mean subsidence rate of a land-use class. Lowest mean subsidence rates are found for natural, undeveloped areas, i.e. marshland and wetland forest, and highest rates for areas with high anthropogenic influence, i.e. mixed-crop agriculture and densely urbanized areas. More anthropogenic impact thus results in higher subsidence rates.

The lowest subsidence rate of 6 mm yr^{-1} occurs in undeveloped marshland. As natural marshland experiences no distinct human influence that alters the hydrological situation or loading of the land surface, this value likely reflects the mean natural compaction rate in the Vietnamese Mekong delta. The same value of 6 mm yr^{-1} was measured as mean floodplain sedimentation rate in frequently flooded areas in the delta (Hung et al., 2014). The similarity of these values probably reflects the dynamic equilibrium between natural compaction and sedimentation in the Mekong delta, which enabled the delta to maintain its

Table 4
Land use and land-use changes: 1996 and 2006. Area is color-coded from green (small) to red (large) and given in percentage of the total study area excluding cloud-covered areas. Land use remained unchanged in 53% of the study area (*in italic* the percentage of unchanged land-use area). Blank spaces show land-use changes that did not happen.

		Aqua-culture	Dry-s. rice	Dry-s. p. rice	Dry-s. b. field	Mix c. no rice	Mangroves	Wet. Forest	Orchard	Urban dense	Urban open	Linear Settle.	Water	Marsh-land	Total in 1996
								Land-use class in 2006							
Land-use class in 1996	Aquaculture	*3.5*				0.1	0.2		0.1			0.1	0.1		4.0
	Dry-season rice	0.0	*19.3*	3.9	3.0	0.1	0.0	0.5	3.2	0.0	0.0	2.5	0.0		32.6
	Dry-season partly rice	0.1	1.0	*0.7*	0.6	0.1	0.0	0.1	0.5	0.0	0.0	0.4	0.0		3.4
	Dry-season bare field	0.8	1.6	1.0	*4.9*	0.3	0.0	0.1	0.4	0.0		0.6	0.0	0.0	9.6
	Mix crops - non-rice	0.1	0.1	0.4	0.2	*0.7*		0.0	0.3	0.0	0.0	0.1	0.0		1.9
	Mangroves	1.5	0.1	0.2	0.1	0.2	*0.3*		0.2	0.0		0.1	0.0		2.5
	Wetland forest	0.0	0.6	0.0	0.0	0.0		*0.8*	0.3			0.2	0.0	0.0	1.9
	Orchard	0.6	4.0	3.9	1.1	0.4	0.1	0.4	*13.8*	0.1	0.0	2.5	0.2	0.0	27.1
	Urban dense	0.0	0.0	0.0	0.0	0.0		0.0	0.0	*0.1*	0.0	0.0			0.2
	Urban open		0.0	0.0	0.0	0.0		0.0	0.0	0.1	*0.0*	0.0	0.0		0.2
	Linear settlement	0.0	1.3	0.5	0.2	0.0		0.2	0.4	0.0		*1.7*	0.0	0.0	4.5
	Water	0.3	0.1	0.1	0.0	0.0	0.1	0.0	0.1	0.0		0.2	*6.9*		7.9
	Marshland	0.0	0.8	0.1	0.1	0.3		2.0	0.5			0.3	0.0	*0.1*	4.2
	Total in 2006	6.9	28.9	10.7	10.2	2.2	0.7	4.0	19.7	0.5	0.1	8.7	7.4	0.1	100.0
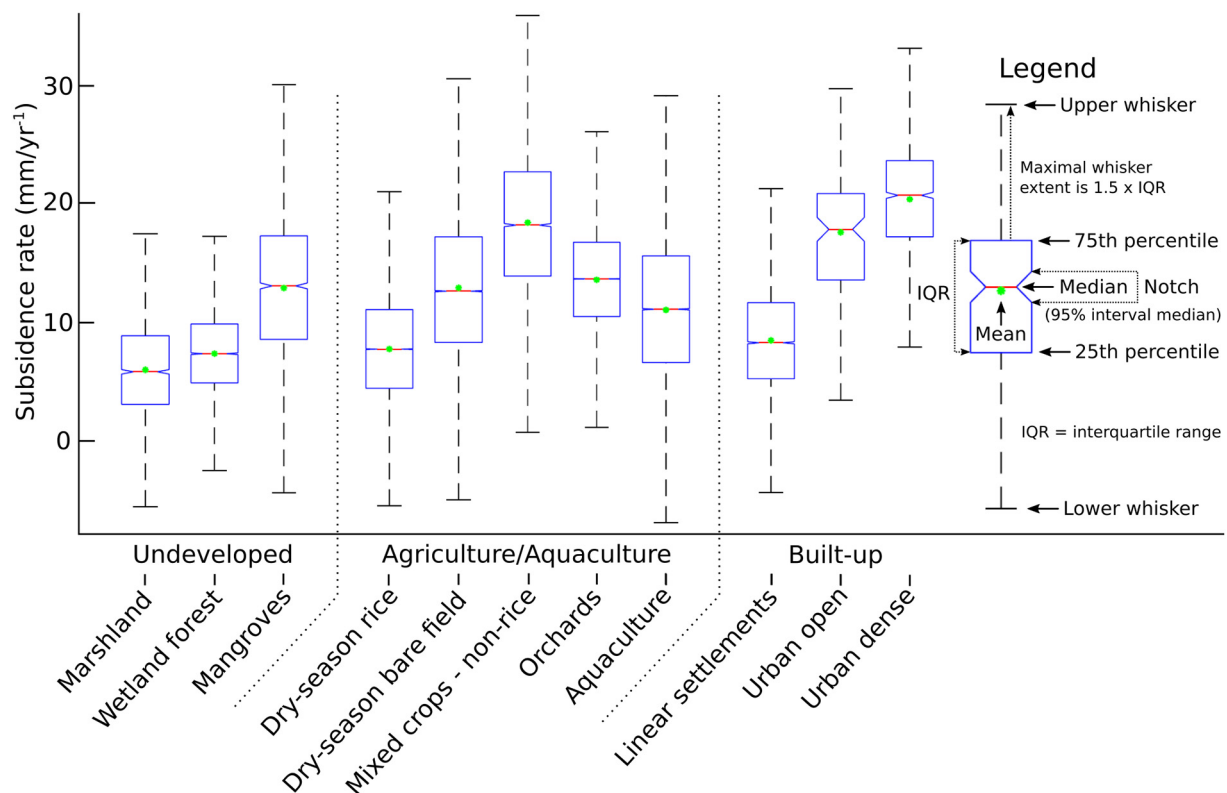
Fig. 3. Subsidence rates (2006–2010) for unchanged land-use sequences during the period 1988–2006. Boxplots summarize the rates for each land-use class. Outliers beyond the whisker range are not shown.

elevation throughout the thousands of years prior to extensive human impact on the delta.

The subsidence rates presented reflect rates of subsidence of solid surfaces, as InSAR is unable to detect sediment accumulation that might occur in wetland areas. For this reason, the subsidence rates of this study may not necessarily reflect net surface-elevation change in some areas and for some land-use classes. For example, mangrove areas experienced relatively high absolute subsidence rates, but sedimentation in those areas can easily be as high or even higher, resulting in a net elevation gain. The latter is actually the case in the Mekong delta as Surface Elevation Table (SET) measurements in mangrove areas registered a net elevation gain in healthy mangrove areas (Lovelock et al., 2015). However, the InSAR subsidence data do not represent elevation changes in these natural land surfaces due to detection limitations, as they only include "hard" reflectors, such as buildings and roads. These are typically objects that likely do not experience elevation gain owing

to sediment deposition. Conversely, the effective dike system, which was constructed to retain irrigation water to enable year-round rice cultivation (dry-season rice), likely decreases the amount of river flood-carried sedimentation, in contrast to more traditional rice cultivation practices (dry-season bare field) that continue to receive sediment by flood pulses. Estimates of the actual surface elevation change for a specific land-use class thus should consider the effect of sediment accumulation as well.

In the agricultural areas, subsidence rates are lowest for "dry-season rice" (irrigated rice). This might be explained by the effect of irrigation during the dry season, resulting in a year-round high phreatic water table. This artificially high phreatic water table prevents soil ripening and organic matter decay in the subsurface, processes that would otherwise induce subsidence during the dry season when the water table normally drops. Other, rain-fed, agricultural land-use types do not have this "paddy benefit" and show higher subsidence rates. A similar

Table 5
Impact of past land-use (LU) changes on the subsidence rates in the Mekong delta. The mean subsidence rates (in mm yr^{-1}) for areas in which LU 1 and LU 2 was unchanged during the period 1988–2006 (columns 'Unchanged LU 1' and 'Unchanged LU 2') and for areas that experienced a transition from LU 1 to LU 2 between 1996 and 2006 (column 'Transition from LU 1 to LU 2 1996–2006') and 1988–1996 (column 'Transition from LU 1 to LU 2 1988–1996'), respectively <10 and 10–18 years before the measurement period (2006–2010). Subsidence rates are color-coded from yellow (low rates) to red (high rates).

|	Land use change		Subsidence rate (mm yr⁻¹)			
	Original land use	Land use after change	Unchanged	Transition from LU 1 to LU 2		Unchanged
Development	*Land use 1*	*Land use 2*	*LU 1*	1996-2006	1988-1996	*LU 2*
Cultivating undeveloped land	Marshland	Dry-season rice	6	8	8	8
	Marshland	Linear settlement	6	8	8	9
	Marshland	Dry-season bare	6	9	10	13
	Marshland	Orchard	6	9	11	14
	Mangroves	Aquaculture	13	11	11	11
Changing agriculture	Dry-season bare	Dry-season rice	13	10	8	8
	Dry-season rice	Orchard	8	10	12	14
Urbanization	Dry-season rice	Urban dense	8	9	27	20
	Dry-season bare	Urban dense	13	16	23	20
	Orchard	Urban dense	14	16	20	20
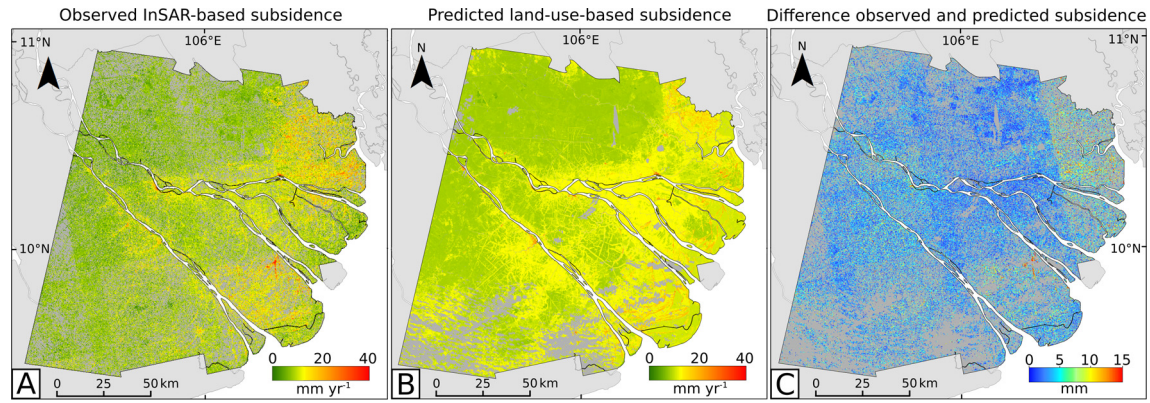
Fig. 4. A) Observed InSAR-based subsidence rate, B) predicted subsidence rates for the period 2006–2010, and C) difference between observed and predicted subsidence. The predicted subsidence over the period 2006–2010 (B) is based on land-use history. Land-use sequence-specific median InSAR-derived subsidence rates were assigned to each individual land-use sequence. Respectively, 66% to 92% of the estimations fall within 5 to 10 mm of the observed values, which corresponds to the error range associated with the InSAR-based subsidence observations (A).

difference was observed in Japan where land subsidence rates in areas with rain-fed upland crops (comparable to our class 'mixed crop - non rice') were much higher than for rice paddies (Miyaji et al., 1995). The large difference in mean subsidence rate between rain-fed and irrigated rice thus suggests a high impact of seasonal water table lowering as driver of shallow subsidence.

Groundwater extraction causes differences in subsidence rates between the various agricultural land-use classes. While Vietnamese law prohibits groundwater extraction for rice irrigation, this seems to be tolerated for the irrigation of mixed crops and orchards. Moreover, rice paddies irrigated by river water potentially increase groundwater recharge to the deeper layers, therefore reducing groundwater extraction-driven subsidence (Wen, 1995), as was observed in Taiwan (Liu et al., 2010). However, we expect this recharging effect to be small in the Mekong delta, due to the thick, clay-rich Holocene top layer, which effectively seals off the underlying, exploited aquifers (Minderhoud et al., 2017).

In densely urbanized areas, subsidence rates are highest. This agrees with observations of rapidly subsiding delta cities elsewhere, such as Bangkok (Phien-wej et al., 2006), Jakarta (Abidin et al., 2011) and Shanghai (Ye et al., 2016). These high subsidence rates are due to the combination of all three main anthropogenic subsidence drivers: effective drainage causing a lowering of the groundwater table, excessive groundwater extraction, and physical loading of the compressible subsurface sediments by city buildings and infrastructure. For rural settlements the subsidence rate is lower, as the above-mentioned drivers are much less intensive. Besides, these settlements often occupy higher elevated terrain, and are often located as linear settlements on natural levees that are less prone to subsidence than flood-basins sediments.

Remarkably high subsidence rates were found for mangrove areas, despite the absence of human interference to accelerate subsidence. Here, the high rates might be attributed to their near-coastal position on the geologically youngest parts of the delta plain (e.g. Ta et al., 2002); these recently deposited, unconsolidated sediments are
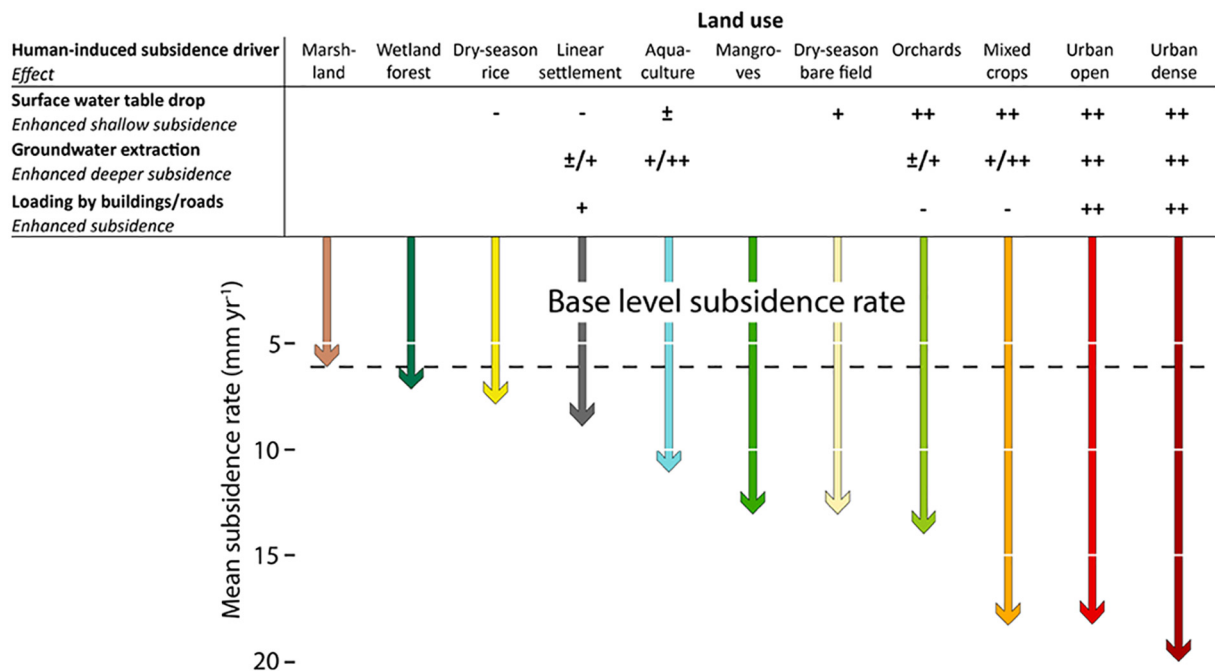
Fig. 5. Estimated impact of subsidence drivers, and mean InSAR-based subsidence rate for the period 2006–2010 per land-use class. Mean subsidence rate is based on areas that sustained the same land use throughout the period of 1988–2006. The estimated impact of each subsidence driver is ranked: minimal ($-$), low ($\pm$), moderate ($+$) and high ($++$). All classes experience a subsidence rate of at least 6 mm yr^{-1}. Higher subsidence rates are generally found for land-use classes associated with increased impact of anthropogenic subsidence drivers.

probably highly susceptible to natural compaction. This observation is in line with the high rates of shallow subsidence measured in the youngest, near-coastal mangrove areas in the Mekong delta (Lovelock et al., 2015).

The relatively low subsidence rates found for areas with aquaculture are remarkable, and contradict observations from other deltas such as the Yellow river delta where groundwater extraction at an aquaculture-dominated coastline causes local annual subsidence rates of several decimeters per year (Higgins et al., 2013). The low subsidence rates for aquaculture in the study area suggest limited groundwater extraction. This is in line with the relatively small groundwater pressure drop and inherent extraction-induced subsidence, documented for the aquaculture areas in the study area for the InSAR observation period (Minderhoud et al., 2017). Probably, the aquacultures in the study area are partly fed by river water from the nearby Mekong river branches. Still, areas with aquaculture in the south of the Mekong delta, outside our study area, seem to experience more groundwater-extraction-induced subsidence (Minderhoud et al., 2017).

4.2.1. Within-class variation of subsidence rate

The standard deviation of observed subsidence rates varies between 4 and 7 mm yr^{-1} for the different land-use classes (SI section S3). Apart from the contribution of InSAR inaccuracy (5–10 mm yr^{-1}; Erban et al., 2013, 2014) and inaccuracies in the land-use classifications, this variation may reflect actual (spatial) variation of subsidence rates present within a certain land-use class.

Within-class variation of subsidence rates may be attributed to four categories of factors: 1) differences in water use and water management within areas with the same land use; 2) "transboundary" subsidence resulting from practices in neighboring areas with a different land use, e.g. groundwater extraction at a single location can influence a much larger area; 3) variability in inherited subsidence related to land use and land-use changes prior to 1988; 4) properties of the physical system that are independent of land use, including local subsurface composition and tectonic subsidence. This last factor is captured by a trend in subsidence rates for the linear settlements land-use class that shows increasing rates from the northwest, upstream part, towards the southeast, downstream part of the delta. This trend likely reveals the higher natural compaction rates associated with the younger, shallow sediments in seaward direction.

4.3. Land-use change and time-dependent subsidence response

Our results show that most of the investigated land-use changes in the Mekong delta led to an acceleration of subsidence rates. Only the conversion from rain-fed rice to year-round irrigated rice and the conversion from mangroves to aquaculture shows reduced subsidence rates. Furthermore, when the land-use conversion occurred in the first period (1988–1996), the present subsidence rate under the new land use is more similar to the characteristic subsidence rate of the unchanged land-use class than when the conversion occurred in the second period (1996–2006). This delayed change in subsidence rate following a land-use change clearly reveals the delayed response or time-lag of subsidence.

This time-lag in subsidence rate is the result of time-dependent effects of which we distinguish two types. 1) Time-dependent effects can stem from changing boundary conditions and the delayed response of subsidence drivers and processes. Examples are the ongoing drainage of land following the conversion to agricultural land resulting in gradually phreatic water table lowering (driver) which leads to increasing clay and peat compaction and peat oxidation (processes), or, a land use changes to a more groundwater-demanding land-use type with increased groundwater exploitation (driver) which leads to increasing rates of aquifer-system compaction (process). 2) The second type of time-dependent effect that we distinguish can stem from internal mechanisms of subsidence processes. Examples are the decrease of

subsidence over time following decomposition of organic matter as organic matter gradually depletes (Yuill et al., 2009), or, in case of aquifer system compaction, the subsidence rate gradually decreases when a new equilibrium between pore pressure and overburden is reached (Isotton et al., 2015). Our results suggest that time-dependent effects can affect subsidence rates up to at least two decades following a land-use change. This underscores the importance of land-use history, and not just current land use, when studying the land use-subsidence relationship.

Finally, it should be noted that the subsidence rates reported and predicted in this study are based on the InSAR analysis of subsidence acquired between 2006 and 2010 (Erban et al., 2014). Given the accelerating trend in groundwater extraction-related subsidence in the Mekong delta (Minderhoud et al., 2017), these rates likely underestimate the present-day subsidence rates. This effect will be especially apparent for land-use classes that require large volumes of groundwater use, e.g. mixed crops, aquaculture and urban areas.

4.4. Predictions of subsidence rates based on land-use history

The observed InSAR-derived subsidence rates and the land-use-based predicted rates agree well and show similar spatial patterns and magnitudes of rate. These spatial patterns are no longer present in the residuals map, which means that a large part of the spatial variability of the InSAR-observed subsidence across the delta is correlated with land-use history. This confirms the existence of the hypothesized relation between land-use history and subsidence, as 1) land-use practices affect subsidence drivers and processes and/or 2) preference of land-use types for locations with specific subsidence characteristics. The majority (65%–92%) of the predicted rates falls within the error range of the observed, InSAR-derived subsidence rates (5–10 mm yr^{-1}). This confirms the possibility of providing predictions of subsidence rate using land-use history when it can be trained using subsidence-rate observations. Incorporating land-use history, and not just land use, to prediction subsidence rates strongly increased the prediction results. Predictions of subsidence rates based on land-use history should therefore preferably be derived from time series of land use covering the longest possible period.

Subsidence predictions could potentially be improved by including additional factors that influence subsidence unrelated to land use, such as subsurface composition, if spatial data is available. In this study, the data used to derive the median values had the same spatial extent for which we predicted subsidence. However, the method might also be applied to create estimations of land-subsidence for regions larger than the training area, as long as the land-use classes and the corresponding dominant subsidence drivers and processes remain similar. In such cases using land-use history as a proxy for subsidence rates provides a promising approach for data-sparse regions lacking direct subsidence measurements, such as large delta systems, to produce subsidence estimates for the entire region using land-use maps. For instance, this approach could be applied in the Ganges-Brahmaputra delta where InSAR-based subsidence data is currently available for a small region only (Higgins et al., 2014).

4.5. Supporting land-use management in subsiding deltas

Our results show a clear link between land use (trajectories) and subsidence in the Mekong delta. These insights may be used to guide sustainable land-use planning that considers delta subsidence and promotes land-use types less prone to subsidence. Additionally, our spatially explicit evaluation can aid policy making and planning around subsidence-mitigation measures. Our approach is further relevant to any area in the world where land-use practices. Using land cover data, which are more readily available than direct or indirect measurements of subsidence, as a proxy for subsidence rates, facilitates such opportunities also in data-sparse deltas and other regions.

5. Conclusions

The Vietnamese Mekong delta has experienced major changes in land use over the past decades. The wide-spread cultivation of previously undeveloped lands and expansion of cities strongly altered the hydrological situation in the delta, both at the surface and in the subsurface, and added loading to the delta plain. These anthropogenic drivers triggered and enhanced subsidence processes. Our analysis of land use and InSAR-derived subsidence rates demonstrates that different land uses lead to different subsidence rates, where more anthropogenic influence leads to higher rates.

In general, subsidence rates in the Mekong delta increase after conversion of land use to a type that uses more groundwater or causes land subsidence otherwise. Past land-use changes, between 1988 and 1996 or 1996–2006, significantly influence subsidence rates observed between 2006 and 2010. This means that both subsidence drivers and processes can need at least up to two decades to adapt to the new land-use practices. Hence it is important to include the land-use history over several decades rather than current land use in the analysis of subsidence rates.

The predicted subsidence rates for the land-use classes and land-use change sequences agree well with the InSAR-derived subsidence rates. This confirms the strong relation between land-use history and subsidence. It also reveals the ability to predict subsidence rates based on land-use history. Moreover, it could provide a promising proxy-approach for upscaling and producing subsidence estimates for larger regions that lack direct subsidence measurements. The relation between land use, land-use history and subsidence rate reveals their strong interlinkage through subsidence drivers and processes caused by the use of land as well as land-use preference for locations with specific subsurface characteristics. Overall, our spatially explicit evaluation of land-use change pathways provides land-use specific insights for policymakers concerned with land-use planning in both subsiding and currently stable areas of the Mekong delta and similar systems.

Acknowledgements

Author contributions

P.M., E.S., and E.A. jointly conceived this research as part of the Rise and Fall research project and supervised the MSc graduation research of L.C. L.C. collected the optical remote sensing data and performed the pre-processing. L.E. performed the InSAR analysis. E.A., L.C., and P.M. designed the remote sensing and machine-learning analyses and P.M., L.C., and E.S. the subsidence analyses. L.C. performed all computer analyses and reported the study in a MSc thesis. P.M. drafted the paper, which was then edited by all co-authors.

Appendix A. Supplementary data

Supplementary data to this article can be found online at https://doi.org/10.1016/j.scitotenv.2018.03.372.

References

Abidin, H.Z., Andreas, H., Gumilar, I., Fukuda, Y., Pohan, Y.E., Deguchi, T., 2011. Land subsidence of Jakarta (Indonesia) and its relation with urban development. Nat. Hazards 59:1753–1771. https://doi.org/10.1007/s11069-011-9866-9.

Addink, E.A., Van Coillie, F.M.B., de Jong, S.M., 2012. Introduction to the GEOBIA 2010 special issue: from pixels to geographic objects in remote sensing image analysis. Int. J. Appl. Earth Obs. Geoinf. 15:1–6 doi:https://doi.org/10.1016/j.jag.2011.12.001.

Anthony, E.J., Brunier, G., Besset, M., Goichot, M., Dussouillez, P., Nguyen, V.L., 2015. Linking rapid erosion of the Mekong River delta to human activities. Sci. Rep. 5, 14745. https://doi.org/10.1038/srep14745.

Binh, T.N.K.D., Vromant, N., Hung, N.T., Hens, L., Boon, E.K., 2005. Land cover changes between 1968 and 2003 in Cai Nuoc, Ca Mau peninsula, Vietnam. Environ. Dev. Sustain. 7:519–536. https://doi.org/10.1007/s10668-004-6001-z.

Blaschke, T., 2010. Object based image analysis for remote sensing. ISPRS J. Photogramm. Remote Sens. 65:2–16. https://doi.org/10.1016/j.isprsjprs.2009.06.004.

Bouvet, A., Le Toan, T., 2011. Use of ENVISAT/ASAR wide-swath data for timely rice fields mapping in the Mekong River Delta. Remote Sens. Environ. 115:1090–1101. https://doi.org/10.1016/j.rse.2010.12.014.

Breiman, L., 2001. Random forests. Mach. Learn. 45:5–32. https://doi.org/10.1017/CBO9781107415324.004.

Breiman, L., Cutler, A., 2003. Random forests manual v4. Tech. Report. UC Berkel.

Brunier, G., Anthony, E.J., Goichot, M., Provansal, M., Dussouillez, P., 2014. Geomorphology Recent morphological changes in the Mekong and Bassac river channels, Mekong delta : The marked impact of river-bed mining and implications for delta destabilisation. Geomorphology 224:177–191. https://doi.org/10.1016/j.geomorph.2014.07.009.

Chen, C.F., Son, N.T., Chang, L.Y., 2012. Monitoring of rice cropping intensity in the upper Mekong Delta, Vietnam using time-series MODIS data. Adv. Sp. Res. 49:292–301. https://doi.org/10.1016/j.asr.2011.09.011.

Darby, S.E., Hackney, C.R., Leyland, J., Kummu, M., Lauri, H., Parsons, D.R., Best, J.L., Nicholas, A.P., Aalto, R., 2016. Fluvial sediment supply to a mega-delta reduced by shifting tropical-cyclone activity. Nat. Publ. Group https://doi.org/10.1038/nature19809.

Dijk, V., Hilderink, H., Rooij, W., Rutten, M., Ashton, R., Kartikasari, K., Lan, V.C., 2013. Land-use change, food security and climate change in Vietnam: a global-to-local modelling approach. LEI Report, pp. 2013–2020.

Erban, L.E., Gorelick, S.M., Zebker, H.A., Fendorf, S., 2013. Release of arsenic to deep groundwater in the Mekong Delta, Vietnam, linked to pumping-induced land subsidence. Proc. Natl. Acad. Sci. U. S. A. 110:13751–13756. https://doi.org/10.1073/pnas.1300503110.

Erban, L.E., Gorelick, S.M., Zebker, H.A., 2014. Groundwater extraction, land subsidence, and sea-level rise in the Mekong Delta, Vietnam. Environ. Res. Lett. 9, 84010. https://doi.org/10.1088/1748-9326/9/8/084010.

Funkenberg, T., Thai Binh, T., Moder, F., Dech, S., 2014. The Ha Tien Plain – wetland monitoring using remote-sensing techniques the Ha Tien Plain – wetland monitoring using remote-sensing techniques. Int. J. Remote Sens. 358:2893–2909. https://doi.org/10.1080/01431161.2014.890306.

Galloway, D.L., Burbey, T.J., 2011. Review: regional land subsidence accompanying groundwater extraction. Hydrogeol. J. 19:1459–1486. https://doi.org/10.1007/s10040-011-0775-5.

Galloway, D.L., Erkens, G., Kuniansky, E.L., Rowland, J.C., 2016. Preface: land subsidence processes. Hydrogeol. J. 24:547–550. https://doi.org/10.1007/s10040-016-1386-y.

Gambolati, G., Teatini, P., 2015. Geomechanics of subsurface water withdrawal and injection. Water Resour. Res. 51:3922–3955. https://doi.org/10.1002/2014WR016841.

Giang, N.V., Hoa, P.V., 2013. Presentation: mangrove forest monitoring using multi-temporal satellite images Case Study in Ben Tre and Tra Vinh provinces. Second Annu. Coast. Forum Build. Coast. Resil. to Clim. Chang. Coast. Southeast Asia.

Giosan, L., Syvitski, J.P.M., Constantinescu, S., Day, J., 2014. Protect the world's deltas. Nature 516, 5–7.

Giri, C., Defourny, P., Shrestha, S., 2003. Land cover characterization and mapping of continental Southeast Asia using multi-resolution satellite sensor data. Int. J. Remote Sens. 24:4181–4196. https://doi.org/10.1080/0143116031000139827.

Gislason, P.O., Benediktsson, J.A., Sveinsson, J.R., 2006. Random forests for land cover classification. Pattern Recogn. Lett. 27:294–300. https://doi.org/10.1016/j.patrec.2005.08.011.

Higgins, S., Overeem, I., Tanaka, A., Syvitski, J.P.M., 2013. Land subsidence at aquaculture facilities in the Yellow River delta, China. Geophys. Res. Lett. 40:3898–3902. https://doi.org/10.1002/grl.50758.

Higgins, S.A., Overeem, I., Steckler, M.S., Syvitski, J.P.M., Seeber, L., Akhter, S.H., 2014. InSAR measurements of compaction and subsidence in the Ganges-Brahmaputra Delta, Bangladesh. J. Geophys. Res. Earth Surf. 119:1310–1321. https://doi.org/10.1002/2014JF003117.

Hung, N.N., Delgado, J.M., Güntner, A., Merz, B., Bárdossy, A., Apel, H., 2014. Sedimentation in the floodplains of the Mekong Delta, Vietnam part II: deposition and erosion. Hydrol. Process. 28:3145–3160. https://doi.org/10.1002/hyp.9855.

Huth, J., Kuenzer, C., Wehrmann, T., Gebhardt, S., Tuan, V.Q., Dech, S., 2012. Land cover and land use classification with TWOPAC: towards automated processing for pixel- and object-based image classification. Remote Sens. 4:2530–2553. https://doi.org/10.3390/rs4092530.

Isotton, G., Ferronato, M., Gambolati, G., Teatini, P., 2015. On the possible contribution of clayey inter-layers to delayed land subsidence above producing aquifers. Proc. Int. Assoc. Hydrol. Sci. 372:519–523. https://doi.org/10.5194/piahs-372-519-2015.

Karila, K., Nevalainen, O., Krooks, A., Karjalainen, M., Kaasalainen, S., 2014. Monitoring changes in rice cultivated area from SAR and optical satellite images in Ben Tre and Tra Vinh provinces in mekong delta, Vietnam. Remote Sens. 6:4090–4108. https://doi.org/10.3390/rs6054090.

Kondolf, G.M., Rubin, Z.K., Minear, J.T., 2014. Dams on the Mekong: cumulative sediment starvation. Water Resour. Res. 50:5158–5169. https://doi.org/10.1002/2013WR014651.

Kono, Y., 2001. Canal development and intesification of rice cultivation in the Mekong Delta: a case study in the Cantho province, Vietnam. Southeast Asian Stud. 39, 70–85.

Kuenzer, C., Knauer, K., 2013. Remote sensing of rice crop areas. Int. J. Remote Sens. 34: 2101–2139. https://doi.org/10.1080/01431161.2012.738946.

Kuenzer, C., Bluemel, A., Gebhardt, S., Quoc, T.V., Dech, S., 2011. Remote sensing of mangrove ecosystems: a review. Remote Sens. https://doi.org/10.3390/rs3050878.

Kummu, M., Varis, O., 2007. Sediment-related impacts due to upstream reservoir trapping, the lower Mekong River. Geomorphology 85:275–293. https://doi.org/10.1016/j.geomorph.2006.03.024.

Liu, C.-W., Zhang, S.-W., Lin, K.-H., Lin, W.-T., 2010. Comparative analysis of temporal changes of multifunctionality benefit of two major rice paddy plains in Taiwan. Paddy Water Environ. 8, 199–205.

Lovelock, C.E., Cahoon, D.R., Friess, D.A., Guntenspergen, G.R., Krauss, K.W., Reef, R., Rogers, K., Saunders, M.L., Sidik, F., Swales, A., Saintilan, N., Thuyen, L.X., Triet, T., 2015. The vulnerability of indo-Pacific mangrove forests to sea-level rise. Nature 526 559–U217. https://doi.org/10.1038/nature15538.

Minderhoud, P.S.J., Erkens, G., Pham, V.H., Vuong, B.T., Stouthamer, E., 2015. Assessing the potential of the multi-aquifer subsurface of the Mekong Delta (Vietnam) for land subsidence due to groundwater extraction. Proc. Int. Assoc. Hydrol. Sci. 372:73–76. https://doi.org/10.5194/piahs-372-73-2015.

Minderhoud, P.S.J., Erkens, G., Pham Van, H., Bui Tran, V., Erban, L.E., Kooi, H., Stouthamer, E., 2017. Impacts of 25 years of groundwater extraction on subsidence in the Mekong delta, Vietnam. Environ. Res. Lett. 12. https://doi.org/10.1088/1748-9326/aa7146.

Miyaji, N., Kohyama, K., Otsuka, H., Kasubuchi, T., 1995. Surface subsidence of peatland in Bibai, central Hokkaido [Japan]. Jap. J. Soil Sci. Plant Nutr. 66 (5), 465–473.

Nguyen, T.T.H., De Bie, C.A.J.M., Ali, A., Smaling, E.M.A., Chu, T.H., 2012. Mapping the irrigated rice cropping patterns of the Mekong delta, Vietnam, through hyper-temporal SPOT NDVI image analysis. Int. J. Remote Sens. 33:415–434. https://doi.org/10.1080/01431161.2010.532826.

Phien-wej, N., Giao, P.H., Nutalaya, P., 2006. Land subsidence in Bangkok, Thailand. Eng. Geol. 82:187–201. https://doi.org/10.1016/j.enggeo.2005.10.004.

Phuong, N.M., Catacutan, D., 2014. Land use Change Analysis in Dien Bien, Son La and Lai Chau Provinces, Northwest Vietnam, for the Period 2000–2010.

Renaud, F.G., Le, T.T.H., Lindener, C., Guong, V.T., Sebesvari, Z., 2015. Resilience and shifts in agro-ecosystems facing increasing sea-level rise and salinity intrusion in Ben Tre Province, Mekong Delta. Clim. Chang. 133:69–84. https://doi.org/10.1007/s10584-014-1113-4.

Rodriguez-Galiano, V.F., Ghimire, B., Rogan, J., Chica-Olmo, M., Rigol-Sanchez, J.P., 2012. An assessment of the effectiveness of a random forest classifier for land-cover classification. ISPRS J. Photogramm. Remote Sens. 67:93–104. https://doi.org/10.1016/j.isprsjprs.2011.11.002.

Sakamoto, T., Van Nguyen, N., Ohno, H., Ishitsuka, N., Yokozawa, M., 2006. Spatiotemporal distribution of rice phenology and cropping systems in the Mekong Delta with special reference to the seasonal water flow of the Mekong and Bassac rivers. Remote Sens. Environ. 100:1–16. https://doi.org/10.1016/j.rse.2005.09.007.

Sakamoto, T., Van Phung, C., Kotera, A., Nguyen, K.D., Yokozawa, M., 2009. Analysis of rapid expansion of inland aquaculture and triple rice-cropping areas in a coastal area of the Vietnamese Mekong Delta using MODIS time-series imagery. Landsc. Urban Plan. 92:34–46. https://doi.org/10.1016/j.landurbplan.2009.02.002.

Son, N.T., Chen, C.F., Chen, C.R., Duc, H.N., Chang, L.Y., 2013. A phenology-based classification of time-series MODIS data for rice crop monitoring in Mekong Delta. Vietnam. Remote Sens. 6:135–156. https://doi.org/10.3390/rs6010135.

Son, N.T., Chen, C.F., Chen, C.R., Duc, H.N., Chang, L.Y., 2014. A phenology-based classification of time-series MODIS data for rice crop monitoring in Mekong Delta, Vietnam. Remote Sens. 6:135–156. https://doi.org/10.3390/rs6010135.

Syvitski, J.P.M., Kettner, A.J., Overeem, I., Hutton, E.W.H., Hannon, M.T., Brakenridge, G.R., Day, J., Vörösmarty, C., Saito, Y., Giosan, L., Nicholls, R.J., 2009. Sinking deltas due to human activities. Nat. Geosci. 2:681–686. https://doi.org/10.1038/ngeo629.

Ta, K.T.O., Nguyen, V.L., Tateishi, M., Kobayashi, I., 2002. Holocene delta evolution and sediment discharge of the Mekong. Quat. Sci. Rev. 21, 1807–1819.

Tong, P.H.S., Auda, Y., Populus, J., Aizpuru, M., Blasco, F., Al Habshi, A., 2004. Assessment from space of mangroves evolution in the Mekong Delta, in relation to extensive shrimp farming. Int. J. Remote Sens. 25:4795–4812. https://doi.org/10.1080/01431160412331270858.

Tran, H., Tran, T., Kervyn, M., 2015. Dynamics of land cover/land use changes in the Mekong Delta, 1973–2011: a remote sensing analysis of the Tran Van Thoi District, Ca Mau Province, Vietnam. Remote Sens. 7:2899–2925. https://doi.org/10.3390/rs70302899.

Triet, N.V.K., Dung, N.V., Fujii, H., Kummu, M., Merz, B., Apel, H., 2017. Has dyke development in the Vietnamese Mekong Delta shifted flood hazard downstream? Hydrol. Earth Syst. Sci. Discuss.:1–27 https://doi.org/10.5194/hess-2017-123.

USGS, 2016. LandsatLook Viewer. US Geological Survey. landsatlook.usgs.gov/viewer (accessed 14-11-2016).

Van Asselen, S., Stouthamer, E., Van Asch, T.W.J., 2009. Earth-science reviews effects of peat compaction on delta evolution: a review on processes, responses, measuring and modeling. Earth Sci. Rev. 92:35–51. https://doi.org/10.1016/j.earscirev.2008.11.001.

Vo, Q.T., Oppelt, N., Leinenkugel, P., Kuenzer, C., 2013. Remote sensing in mapping mangrove ecosystems - an object-based approach. Remote Sens. 5:183–201. https://doi.org/10.3390/rs5010183.

Wagner, F., Tran, V.B., Renaud, F.G., 2012. Chapter 7: groundwater resources in the mekong delta: availability, utilization and risks. The Mekong Delta System. In: Renaud, F.G., Kuenzer, C. (Eds.), Groundwater Resources in the Mekong Delta: Availability, Utilization and Risks. Springer Environmental Science and Engineering. Springer Netherlands, Dordrecht:pp. 201–220 https://doi.org/10.1007/978-94-007-3962-8.

Wassmann, R., Hien, N.X., Hoanh, C.T., Tuong, T.P., 2004. Sea level rise affecting the Vietnamese Mekong Delta: water elevation in the flood season and implications for rice production. Clim. Chang. 66:89–107. https://doi.org/10.1023/B:CLIM.0000043144.69736.b7.

Wen, L.J., 1995. Paddy Field, Groundwater and Land Subsidence. American Water Resources Association, Herndon, VA (United States).

Xiao, X., Boles, S., Frolking, S., Li, C., Babu, J.Y., Salas, W., Moore, B., 2006. Mapping paddy rice agriculture in south and Southeast Asia using multi-temporal MODIS images. Remote Sens. Environ. 100:95–113. https://doi.org/10.1016/j.rse.2005.10.004.

Ye, S., Luo, Y., Wu, J., Yan, X., Wang, H., Jiao, X., Teatini, P., 2016. Three-dimensional numerical modeling of land subsidence in shanghai, China. Hydrogeol. J. 24:695–709. https://doi.org/10.1007/s10040-016-1382-2.

Yuill, B., Lavoie, D., Reed, D., 2009. Understanding subsidence processes in coastal Louisiana. J. Coast. Res.:23–36 Sp.Issue. https://doi.org/10.2112/SI54-012.1.intensity.